MANCHESTER 1824
The University of Manchester

Tracing two-neutron halos in N=28 isotones: A three-body adventure

Jagjit Singh

jagjit.singh@manchester.ac.uk

IOP Joint APP, HEP, and NP Conference, Liverpool.

Parallel Session: H, 10.04.2024 (11:00-11:15)

Based on:

Prediction of two-neutron halos in the N=28 isotones ^{40}Mg and ^{39}Na

Jagjit Singh (UoM), J. Casal (Seville), W. Horiuchi (OMU, Osaka), N. R. Walet (UoM), W. Satula (Warsaw)

arXiv:2401.05160 (2024).

Introduction: Weakly-bound neutron-rich systems

MANCHESTER 1824
The University of Manchester

Stable Separation Energy ~ 8 MeV	Weakly-bound Separation Energy~ 0.1-2 MeV

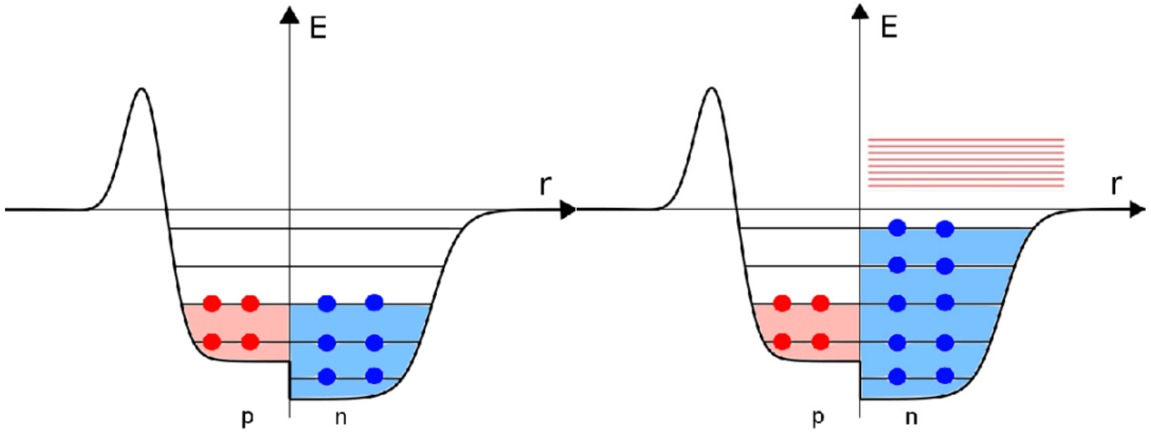

Picture: L. Moschini Master Thesis (ArXiv:1410.7167)

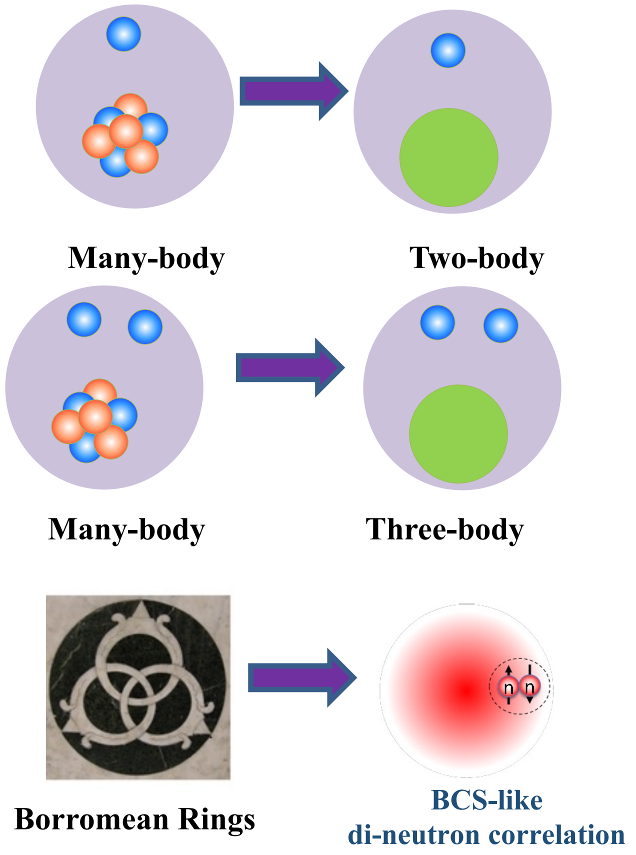

Migdal, Sov. J. Nucl. Phys. 238 (1973).

- Valence nucleon(s) - weakly bound. ^{11}Be (^{10}Be+n) **S_n=0.503** MeV, ^{6}He (^{4}He+n+n) **S_{2n}=0.973** MeV. *P. G. Hansen and B. Jonson, Europhys. Lett. **4**, 409 (1987).*
- Role and treatment of continuum is more significant. ***JS,** PhD thesis, University of Padova (2016).*
- Few-body approaches are convenient tool for such systems. ***JS** et al.,, PRC 101, 024310 (2020).*
- Exotic features such as halo/Borromean formation *I. Tanihata et al., Phys. Rev. Lett., 55 (1985) 2676.*
- Strong short-range cluster like correlation di-neutron - which plays important role in their binding mechanisms leads to weak binding of the system and low-density at the surface. *A.B.Migdal Sov. J. Nucl. Phys. **16**, 238 1973.* *M.Matsuo PRC **73**, 044309 (2006).* *A.Gezerlis, PRC **81**, 025803 (2010).*

MANCHESTER 1824
The University of Manchester

Halo formation on lower Z-side of the magic numbers N=20 and 28

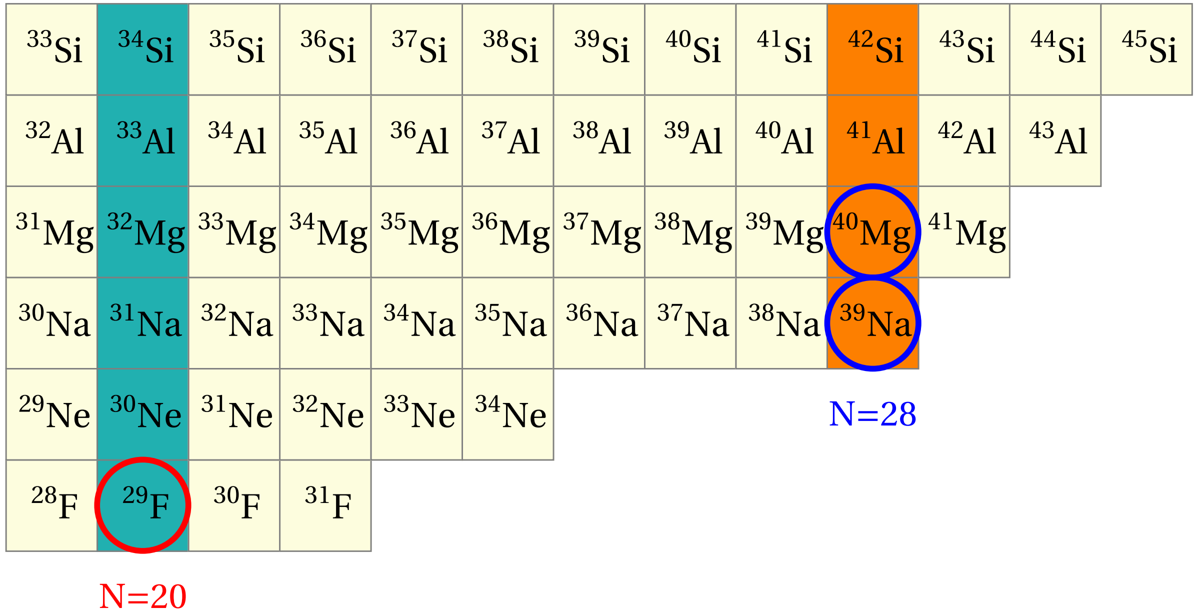

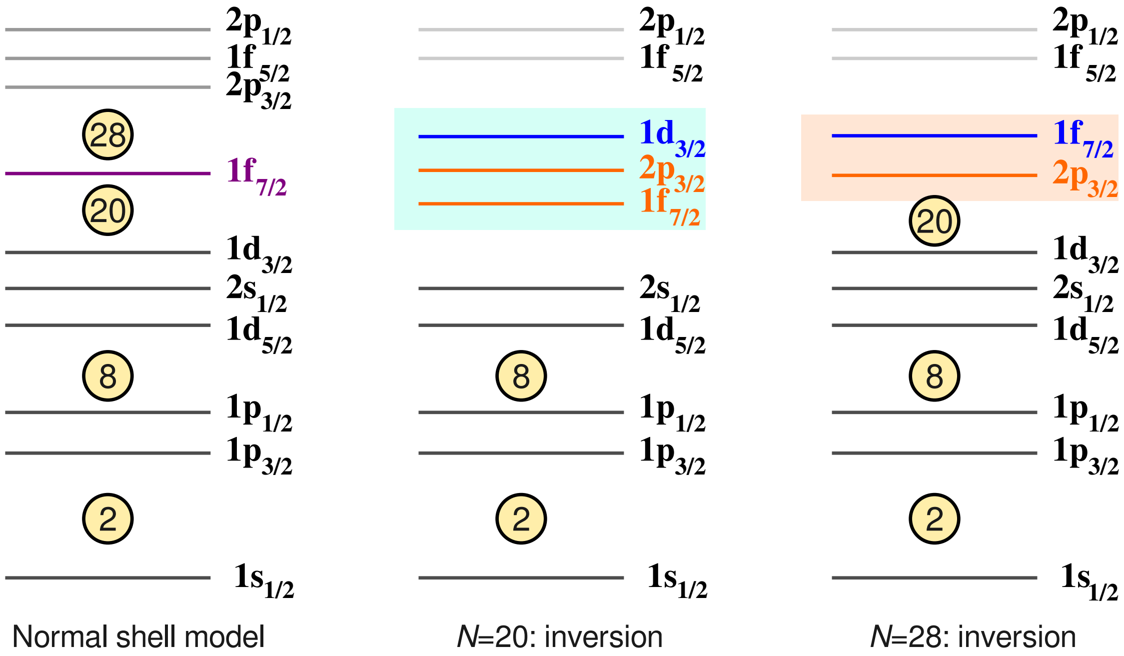

- Recent observation of the disappearance of the **N = 20** shell gap at the low-Z side of the N = 20 chain, led to the identification of the **^{29}F** system as the heaviest known two-neutron Borromean-halo nucleus. *S. Bagchi et al., PRL **124**, 222504 (2020). **JS** et. al., PRC **101**, 024310 (2020). LF, JC, WH, **JS** et. al., Comm. Physics 3, 132 (2020). JC, **JS**, et. al., PRC **102**, 064227 (2020).*

- Motivated by this observation, it is interesting to explore the low-Z side of the N = 28 shell closure for potential two-neutron Borromean halos in the Na and Mg isotopes).

- The $1f_{7/2}$ orbit is bordered by two magic numbers, i.e., 20 and 28. **20** has a HO origin, whereas the **28** has a SO origin.
- Inversion occur, when energy gap, associated with filling of shell closures disappears.

Jagjit Singh et al., arXiv:2401.05160 [nucl- th] (2024).

MANCHESTER 1824
The University of Manchester

Neutron-rich F, Na, and Mg isotopes

^{28}F (Z=9, N=19)
Extending the southern shore of the island of inversion to ^{28}F
*A. Revel et al., PRL **124**, 152502 (2020).*

Unbound
^{27}F+n

-- ground state resonance of ^{28}F at
0.199(6) MeV (l=1~79%)
Inversion !!
-- Ist excited state resonance around
0.966 MeV (l=2~72%)
*PRL **124**, 152502 (2020).*

^{29}F (Z=9, N=20)
*__JS__ ,JC, WH, LF and AV, PRC **101**, 024310 (2020).*
LF, JC, WH, __JS__ and AV, Nature: Communication Physics 3, 132 (2020).
*JC, __JS,__ LF, WH and AV, PRC **102**, 064227 (2020).*
*S. Bagchi et al., PRL **124**, 222504* (2020).

Weakly
Bound
^{27}F+n+n

s_{2n}= 1.443 (436) MeV
=1.440 (650) MeV
PRL. 109, 202503 (2012).
CPCC 41, 030003 (2017).

Tools : Three-body structure model and Glauber reaction theory.

^{40}Mg (Z=12, N=28)
H. L. Crawford et al. Phys. Rev. Lett. 122, 052501 (2019).
T. Baumann et al., Nature volume 449, 1022 (2007).
A. O. Macchiavelli, et al., Eur. Phys. J. A 58, 66 (2022).

Weakly
Bound
^{38}Mg+n+n

s_{2n}= 0.670±0.710 MeV
Chinese Physics C **45 (3)**, 030003 (2021).
No experimental data on ^{39}Mg spectrum
Theoretical predictions within GSM

^{39}Na (Z=11, N=28)
Discovery of 39Na
*D. S. Ahn et al., PRL **129**, 212502 (2022).*
*KY Zhang et al., PRC **107**, L04130303 (2023).*

Weakly
Bound
^{37}Na+n+n

No data on ^{38}Na spectrum
and $s_{2n}$of ^{39}Na.

MANCHESTER 1824
The University of Manchester

Three-Body Structure Model- Hyperspherical framework

PHYSICAL REVIEW C **102**, 064627 (2020)

Three-body Hamiltonian is given by

$$H = T + \sum_{i=1}^{2} V_{core+n_i} + V_{nn} + V_{3b}$$

$$V_{core+n_i} = \left(-V_0 + V_{ls}\vec{l}\cdot\vec{s}\frac{1}{r}\frac{d}{dr}\right)\frac{1}{1+\exp\left(\frac{r-R}{a}\right)},\qquad V_{3b}(\rho) = v_{3b}e^{-(\rho/\rho_o)^2},$$

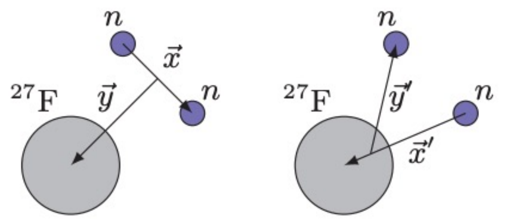

FIG. 1. Jacobi-T (left) and -Y (right) coordinates for the ^{29}F nucleus described as ^{27}F $+n+n$.

nn interaction- Gogny-Pires-Tourreil (GPT) interaction including central, spin-orbit and tensor terms.
D. Gogny, P. Pires, and R. D. Tourreil, PLB ***32****, 591 (1970).*

The three-body force is modelled as a simple Gaussian potential, where ρ= $\sqrt{x^2+y^2}$, is **hyper-radius** and ρ_0=6 fm and the strength v_{3b} is adjusted to recover s_{2n}.

We use the analytical transformed harmonic oscillator (THO) basis.
J. Casal, M. Rodrguez-Gallardo, and J. M. Arias, Phys. Rev. C ***88****, 014327 (2013).*

The diagonalization of the three-body Hamiltonian requires the computation of the corresponding kinetic energy & potential matrix elements.

J. Casal, "Weakly-bound three-body nuclear systems: Structure, reactions and astrophysical implications," Ph.D. thesis, Universidad de Sevilla (2016).

MANCHESTER 1824
The University of Manchester

Reaction cross-section within Glauber model

The reaction cross section for a projectile-target collision integrating the reaction probability with respect to the impact parameter b

Y. Ogawa et al., Prog. Theor. Phys. Suppl. ***142****, 157 (2001a)*

$$\sigma_{\mathrm{R}} = \int d\boldsymbol{b}\left(1 - |e^{i\chi(\boldsymbol{b})}|^2\right),$$

Phase shift function

$$e^{i\chi(\boldsymbol{b})} = \langle \Phi_0^P \Phi_0^T | \prod^{A_P} \prod^{A_T} \left[1 - \Gamma_{NN}(\boldsymbol{s}_i^P - \boldsymbol{s}_j^T + \boldsymbol{b})\right] | \Phi_0^P \Phi_0^T \rangle$$

Profile function $$\Gamma_{NN}(\boldsymbol{b}) = \frac{1 - i\alpha}{4\pi\beta}\sigma_{NN}^{\mathrm{tot}} \exp\left(-\frac{b^2}{2\beta}\right)$$

α, β: determined so as to reproduce the NN scattering

B. Abu-Ibrahim et al., PRC 77, 034607 (2008). W. Horiuchi et al., PRC 75, 044607 (2007).

Phase-shift function: Many-body operator

Approximate using a cumulant expansion: Nucleon-Target profile function

→ Input: **Nuclear density and Profile function no adjustable parameters**

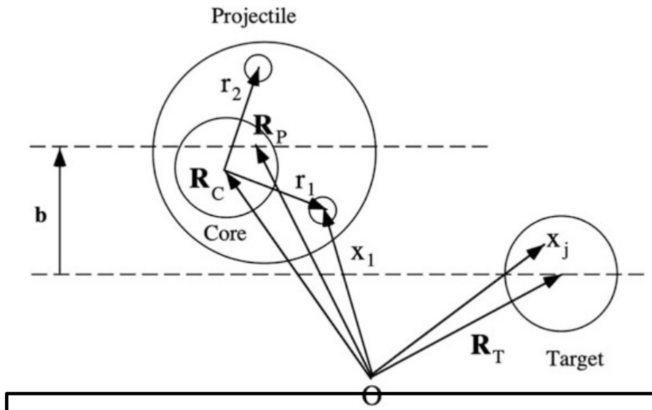

- $r_i = (s_i, z_i)$ is the coordinate of the two-halo neutron(s) with index $i = 1, 2$.
- R_C, R_p, and R_T are the position vectors to the COM of the core nucleus, projectile nucleus, and target nucleus, respectively. $x_i - R_C = r_i$.
- s_i and s_j are the two-dimensional vectors of the coordinates for the P and T, measured from their COM which lies on a plane perpendicular to the incident momentum of the projectile

MANCHESTER 1824
The University of Manchester

Two-body (core+n) models for ^{39}Mg and ^{38}Na

Jagjit Singh et al., arXiv:2401.05160 [nucl- th] (2024).

K. Fossez, *et. al.*, PHYSICAL REVIEW C **94**, 054302 (2016).

Unbound ground state of ^{39}Mg is predicted to be either a ***J^π^* = 7/2^-^ or 3/2^-^ state.**

A narrow $J^{\pi} = 7/2^{-}$ or $3/2^{-}$ ground-state candidate exhibits a resonant structure at 129 KeV.

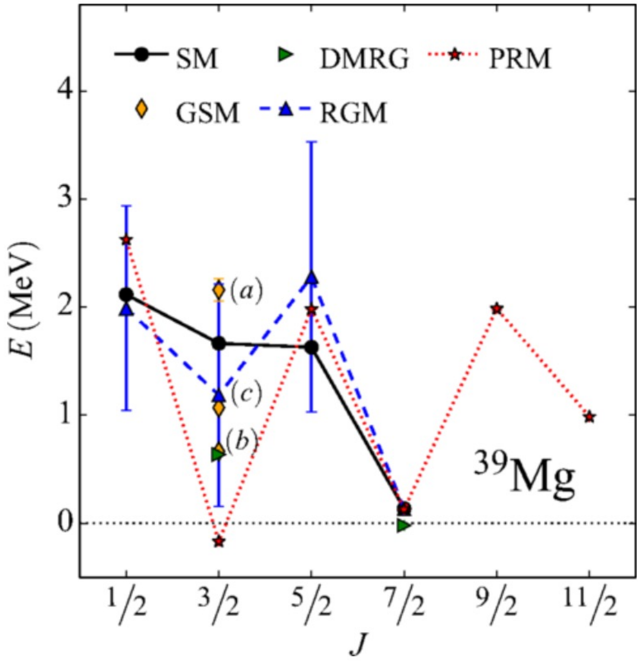

Table 1: Parameter sets for the ^{38}Mg + n (upper-panel) and ^{37}Na + n (lower-panel) Woods-Saxon interactions, Eq. (6). Here a is diffuseness, $V_0^{(l)}$ is the potential depth and E_R is the position of the resonances. Note that r_0 = 1.25 fm, and V_{ls} = 16.842 MeV (for ^{38}Mg + n) and 16.324 MeV (for ^{37}Na + n) are fixed.

Set	Scenario	a (fm)	lj	$V_0^{(l)}$ (MeV)	E_R (MeV)
		^{38}Mg + n			
1	Normal	0.70	$f_{7/2}$	38.225	0.129
			$p_{3/2}$	38.225	0.349
2	Degenerate	0.75	$f_{7/2}$	38.400	0.129
			$p_{3/2}$	38.400	0.135
3	Inverted	0.75	$f_{7/2}$	37.880	0.349
			$p_{3/2}$	38.425	0.130
		^{37}Na + n			
1	Degenerate	0.70	$f_{7/2}$	38.225	0.539
			$p_{3/2}$	38.225	0.599
2	Inverted	0.75	$f_{7/2}$	38.400	0.522
			$p_{3/2}$	38.400	0.271
3	Inverted	0.75	$f_{7/2}$	37.880	0.734
			$p_{3/2}$	38.425	0.265

Configuration mixing and matter radii for ^{40}Mg and ^{39}Na

^{40}Mg (s_{2n}) = 0.670 (0.710) MeV

M. Wang, *et. al.,* Chinese Physics C **45 (3)**, 030003 (2021).

Matter radius of core **^{38}Mg**=3.60 fm

S. Watanabe, *et. al.,* PRC **89,** 044610 (2014).

^{39}Na (s_{2n}) = unbound

M. Wang, *et. al.,* Chinese Physics C **45 (3)**, 030003 (2021).

^{39}Na (s_{2n}) = bound (Contradicts AME)

*D. S. Ahn et al., PRL **129**, 212502 (2022).*

Matter radius of core **^{37}Na**=3.64 fm

L. Geng, *et. al.,* NPA **730**, 80 (2004).

The larger change in R_m *w.r.t* core involves wave function which contains significant $(p_{3/2})^2$ (dotted lines) weight, pointing toward the necessity of intruder configurations to sustain halo formation. $(f_{7/2})^2$ (solid lines)

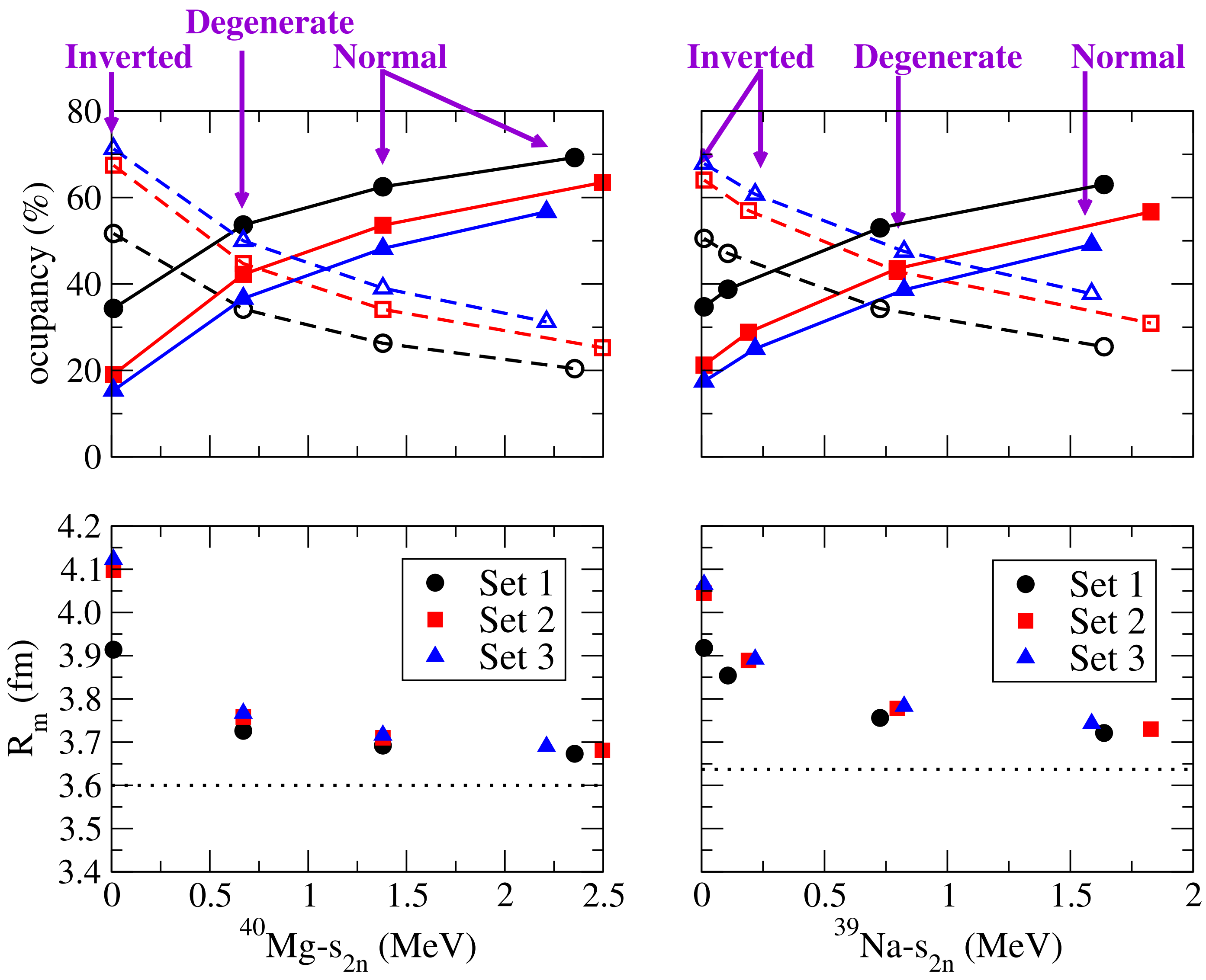

Jagjit Singh et al., arXiv:2401.05160 [nucl- th] (2024).

Matter radii for ^{40}Mg and ^{39}Na

- Dotted black lines in the figure correspond to the weighted fit of the experimental data points with the standard $R_0 A^{1/3}$ formula.
- The radii of ^{40}Mg and ^{39}Na are higher than the standard fitted value.
- This observation implies a likely two-neutron halo structure in the ground state of ^{40}Mg and ^{39}Na, and the corresponding melting of the traditional N = 28 shell gap is due to the intrusion of the $p_{3/2}$ orbital.

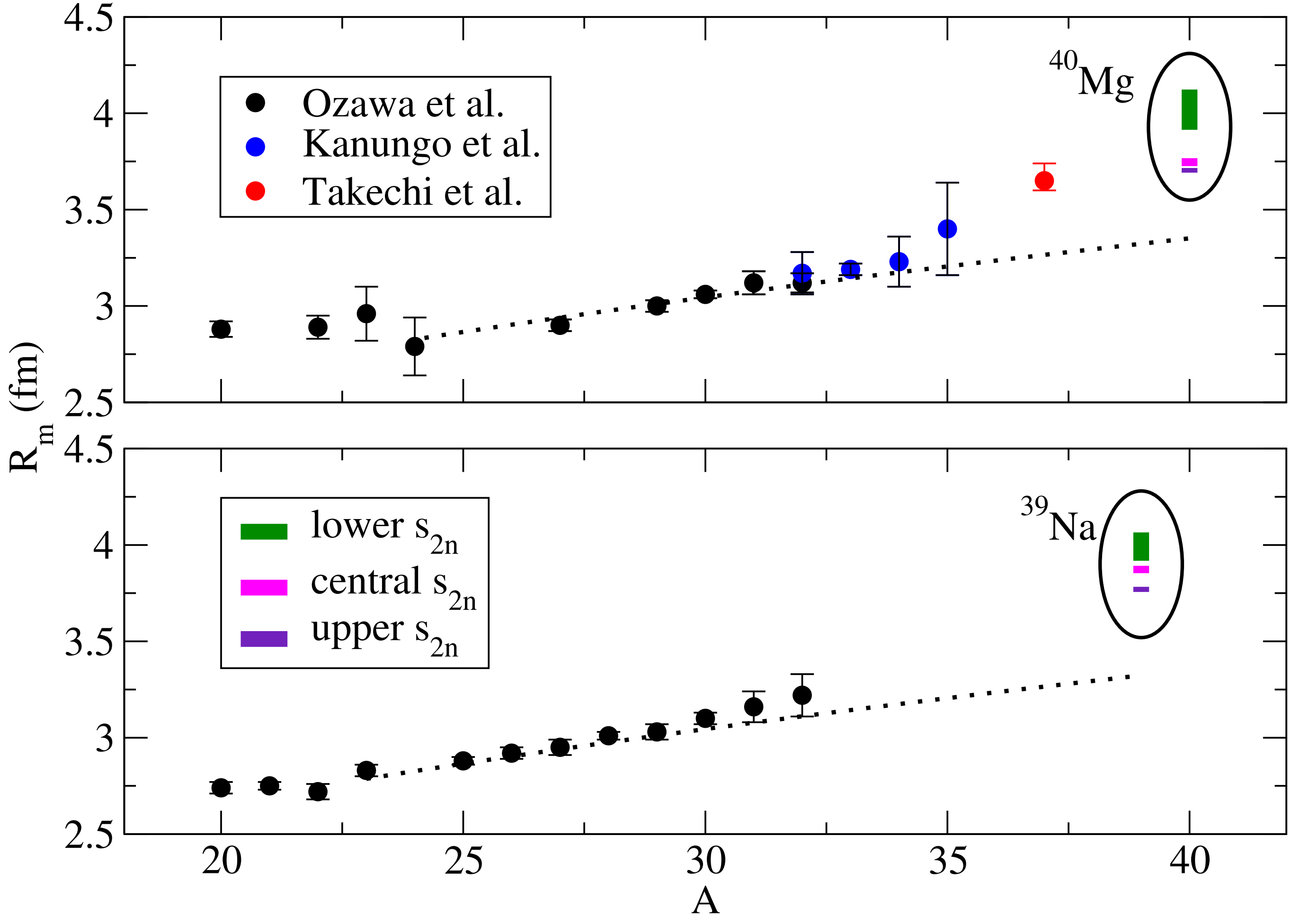

- Ozawa *et al.*, Nuclear Physics A **691 (3)**, 599 (2001).
- Kanungo *et al.*, Phys. Rev. C **83**, 021302 (2011).
- Takechi *et al.*, Phys. Rev. C **90**, 061305(R) (2014).
- *Jagjit Singh et al., arXiv:2401.05160 [nucl- th] (2024).*

Reaction cross-sections for ^{40}Mg and ^{39}Na : within Glauber reaction theory

- Experimentally, a very obvious way to determine whether a nucleus is a halo nucleus, is to look for an enhanced reaction cross section. Thus, we examine the total reaction cross section by employing the conventional Glauber theory. *B. Abu-Ibrahim et al., PRC 77, 034607 (2008). W. Horiuchi et al., PRC 75, 044607 (2007).*

- Using this prescription, we predict the σ_R for ^{40}Mg and ^{39}Na at different incident energies. The predicted values of σ_R for ^{40}Mg and ^{39}Na show significant enhancement with respect to the observed σ_R in the lower-A isotopes for both choices of energy.

Thus, our results provide a clear signal of the 2n-halo structure formation in ^{40}Mg and ^{39}Na and hence melting of the N = 28 shell closure.

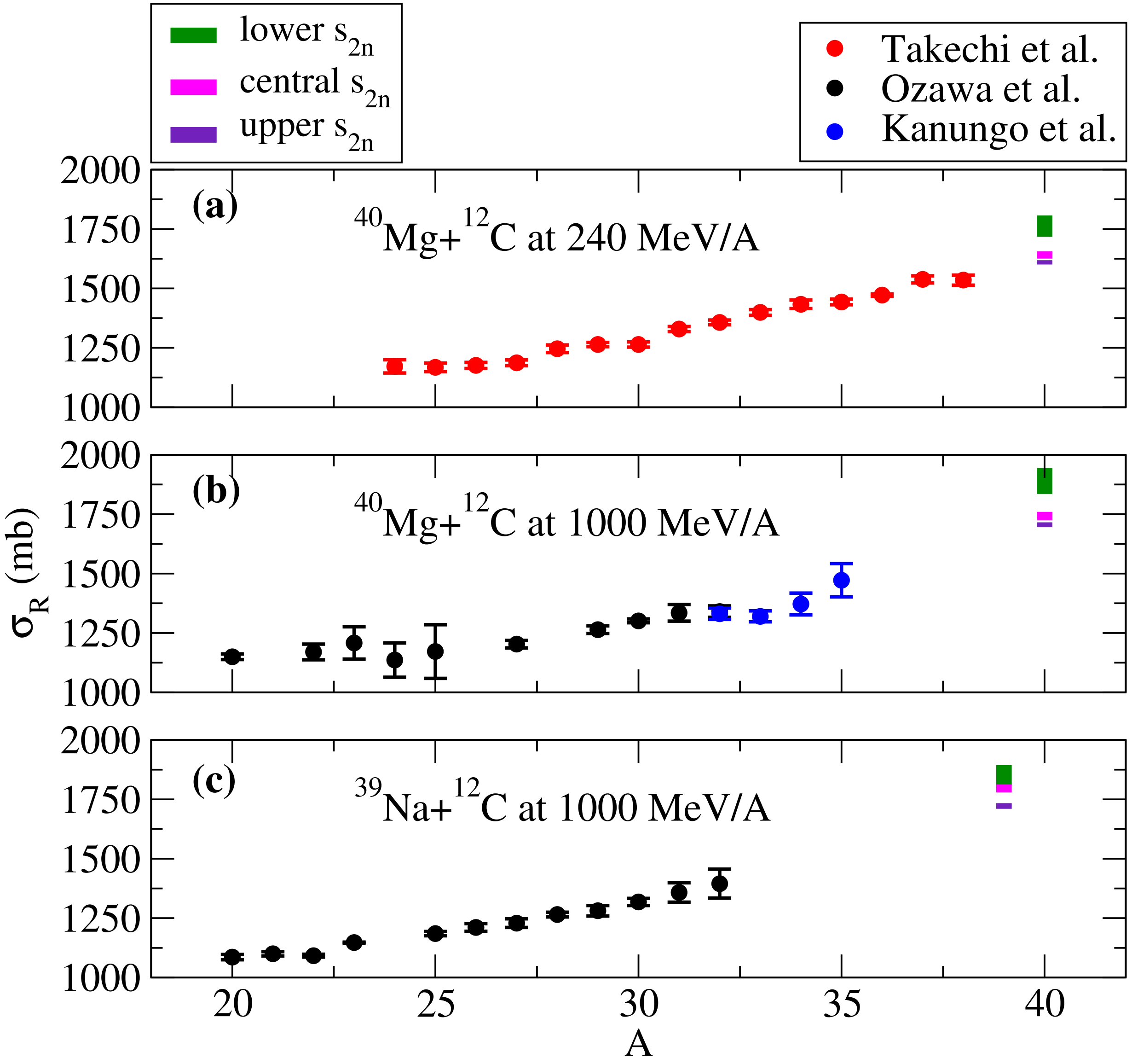

- Ozawa *et al.*, Nuclear Physics A **691 (3)**, 599 (2001).
- Kanungo *et al.*, Phys. Rev. C **83**, 021302 (2011).
- Takechi *et al.*, Phys. Rev. C **90**, 061305(R) (2014).
- *Jagjit Singh et al., arXiv:2401.05160 [nucl- th] (2024).*

MANCHESTER 1824
The University of Manchester

Summary:

- We started with studying melting of N=20 *(**JS**, JC, WH, LF, and AV, PRC **101**, 024310 (2020))* for ^{29}F. Our predictions got boost with new measurements *(S. Bagchi et al., PRL **124**, 222504 (2020) and A. Revel et al., PRL **124**, 152502 (2020)).* We updated our calculations with precise calculations along with detailed analysis of electric-dipole response and reaction calculations *(LF, JC, WH, **JS**, and AV, Nature: Commun. Phys. **3**, 132 (2020) and JC, **JS**, LF, WH, and AV, PRC **102**, 064627 (2020)).*
- Motivated by melting N=20 ends up in formation of Borromean in ^{29}F, by using same prescription we reported first three body calculations for ^{39}Na and ^{40}Mg lying on low-Z side of N=28. *(**JS**, JC, WH, NW, and WS arXiv:2401.05160 [nucl- th] (2024)),*
- Our results calls for new precise mass measurements for s_{2n} of three-body systems and the low-lying continuum spectrum of subsystems to better constrain the theoretical models.
- The disappearance of the conventional N=28 shell gap and emergence of the halo leads to significant occupancy of intruder $p_{3/2}$ orbit in the ground state of ^{39}Na and ^{40}Mg. Nevertheless, it is imperative to verify this conclusion through experimental measurements of interaction cross sections.

Future Perspectives:

- It is interesting to see how our predictions/results alter with inclusion of core deformation effects.

MANCHESTER 1824
The University of Manchester

Thanks for kind attention.

Acknowledgements:
J. Casal (Seville)
W. Horiuchi (OMU, Osaka)
N. R. Walet (Manchester)
W. Satula (Warsaw)
L. Fortunato (Padova)
A. Vitturi (Padova)

The University of Manchester

Key features of halo nuclei

- **Halo nuclei (manifestation of nuclear clustering)** exhibit: a *diffuse density distribution*, low one or more valence neutron(s) separation energies (s_n/s_{2n}), *abnormally large matter radius* and *large interaction cross sections*. P. G. Hansen and B. Jonson, Europhys. Lett. **4**, 409 (1987).

- **Borromean systems (2n-halo):** Corresponding ***core+n*** subsystems being unbound, the strong correlations between the valence neutrons are key in binding two-neutron halos M. Zhukov *et. al.*, Phys. Rep. **231**, 151 (1993). Y. Kikuchi *et al.*, PTEP **2016**, 103D03 (2016). Hagino & Sagawa, PRC **72**, 044321 (2005). Observed examples: ^{6}He, ^{11}Li, and ^{14}Be , ^{17}B, ^{19}B, ^{22}C and ^{29}F.

- **Low-lying spectra** of the unbound ***core+n*** subsystems play an important role in shaping the properties of Borromean nuclei. One of the other salient features of halo nuclei is an *enhancement of the low-lying E1 (electric dipole) strength* into the continuum T. Aumann, EPJA **55**, 234 (2019) . Experimentally this has been observed via *invariant mass spectroscopy in Coulomb dissociation (CD) experiments*.

- **Theoretically three-body (*core+n+n*) models** have been found to describe reasonably well these features in *Borromean nuclei*.

R. Kanungo, Handbook of Nuclear Physics (2023).

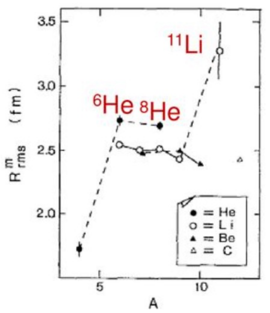

I. Tanihata *et. al.*, PRL **55,** 2676 (1985).

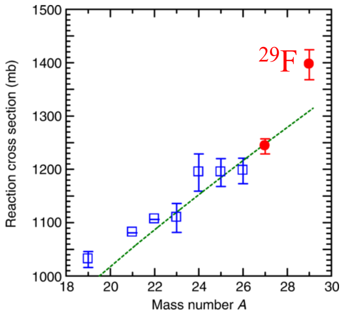

S. Bagchi et al., PRL ***124****, 222504* (2020).

Borromean Rings

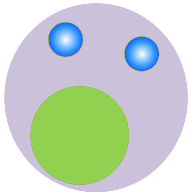

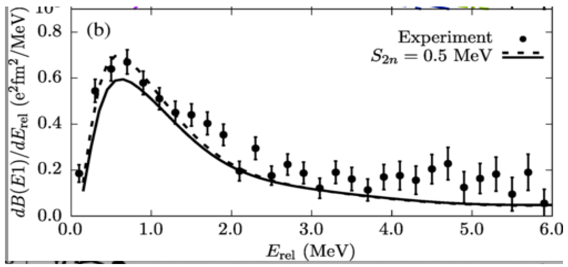

K. Cook *et. al.*, PRL **124**, 212503 (2020).

Key inputs:

- Information on core+n low-lying spectrum
- Two-neutron separation energy

JS *et al.., PRC* ***101****, 024310 (2020).*
JS *et al., arXiv:2401.05160 [nucl- th] (2024).*

Success story of ^{29}F

New Experiment confirms ground state resonance of ^{28}F at 0.199(6) MeV (l=1~79%) and Ist excited state resonance around 0.966 MeV (l=2~72%). **Inversion !!**
*A. Revel et al., PRL **124**, 152502 (2020).*

Total reaction Cross section within Glauber Model
The calculated total reaction cross section using the standard Glauber theory are **1370 mb** if we assume s_{2n} = 1.44 MeV, and **1390 mb** if we take the lower limit ($S_{2n} \approx$ 1 MeV), which are in good agreement with the observed interaction cross section **1396 ± 28 mb.**
*JC, **JS**, et. al., PRC **102**, 064627 (2020).*
s_{2n} (^{29}F) =1.443 (436) MeV *PRL. 109, 202503 (2012).*

Matter radius of $_{29}$F
The relative increase of matter radii with respect to ^{27}F core lies in the range **0.20-0.25** fm in the different choices of s_{2n} whereas experimental value is **0.35 (0.08) fm.**

***JS** ,JC, WH, LF and AV, PRC **101**, 024310 (2020).*

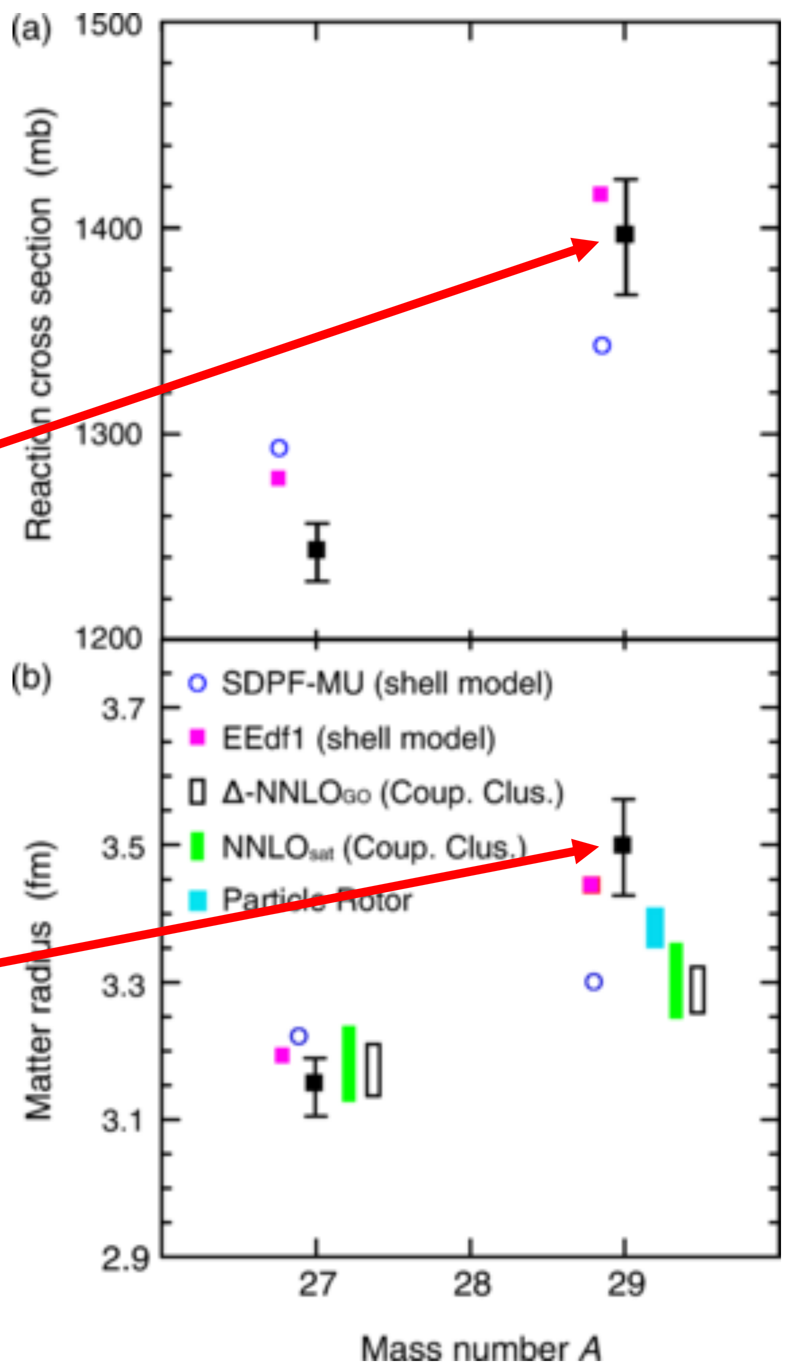

*S. Bagchi et al., PRL **124**, 222504 (2020).*

Background: Inversion mechanism

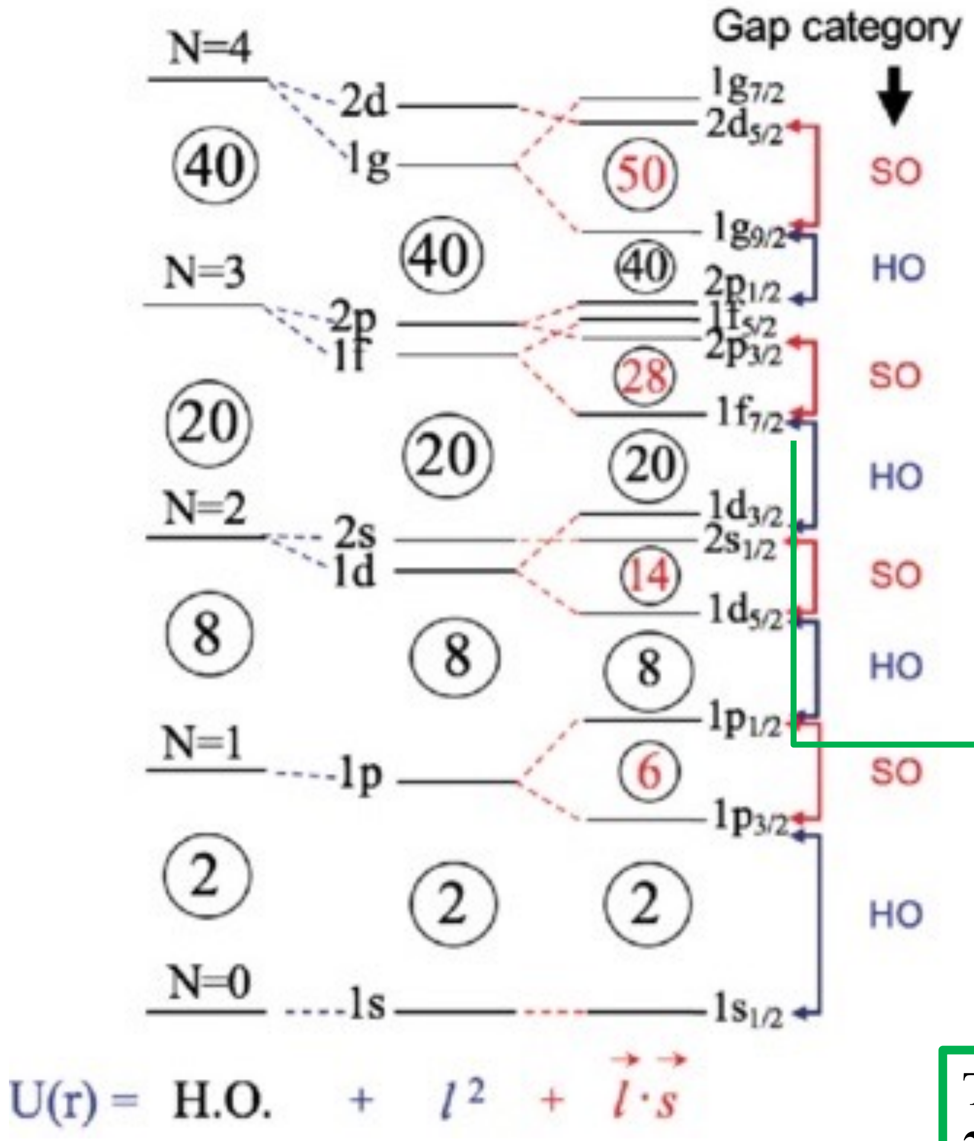

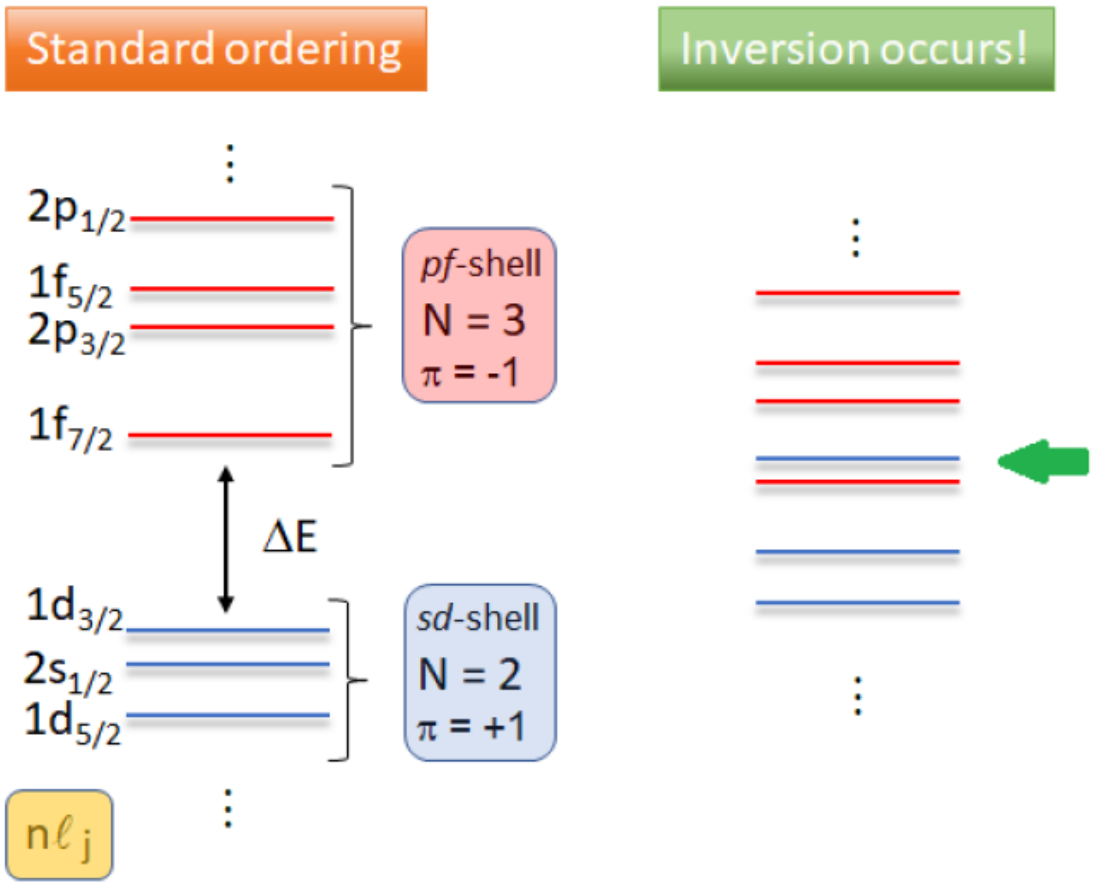

Inversion occur, when ΔE, associated with filling of ***20 neutrons***, disappears and one level (or more) of the ***pf-shell (N = 3)*** gets lower than one (or more) of the levels of the ***sd-shell (N = 2).***

The $1f_{7/2}$ orbit is bordered by two magic numbers, i.e., 20 and 28
20 has a HO origin, whereas the **28** has a SO origin.

T. Otsuka et al., Rev. Mod. Phys. ***92****, 015002 (2020).*

LF, JC, WH, ***JS*** *et. al., Comm. Physics 3, 132 (2020).*